

Dynamic and Compressive Adaptation of Transformers From Images to Videos

Guozhen Zhang^{1,2*}, Jingyu Liu², Shengming Cao², Xiaotong Zhao²,
Kevin Zhao², Kai Ma², and Limin Wang^{1,3†}

¹ State Key Laboratory for Novel Software Technology, Nanjing University

² Platform and Content Group (PCG), Tencent

³ Shanghai AI Lab

Abstract. Recently, the remarkable success of pre-trained Vision Transformers (ViTs) from image-text matching has sparked an interest in image-to-video adaptation. However, most current approaches retain the full forward pass for each frame, leading to a high computation overhead for processing entire videos. In this paper, we present InTI, a novel approach for compressive image-to-video adaptation using dynamic **Inter-frame Token Interpolation**. InTI aims to softly preserve the informative tokens without disrupting their coherent spatiotemporal structure. Specifically, each token pair at identical positions within neighbor frames is linearly aggregated into a new token, where the aggregation weights are generated by a multi-scale context-aware network. In this way, the information of neighbor frames can be adaptively compressed in a point-by-point manner, thereby effectively reducing the number of processed frames by half each time. Importantly, InTI can be seamlessly integrated with existing adaptation methods, achieving strong performance without extra-complex design. On Kinetics-400, InTI reaches a top-1 accuracy of 87.1 with a remarkable 37.5% reduction in GFLOPs compared to naive adaptation. When combined with additional temporal modules, InTI achieves a top-1 accuracy of 87.6 with a 37% reduction in GFLOPs. Similar conclusions have been verified in other common datasets.

Keywords: Image-to-video adaptation · Token interpolation

1 Introduction

Video recognition is attracting significant attention due to its potential for wide applications. As image pre-trained models can provide powerful representations for video understanding [4, 51], image-to-video adaptation has been extensively studied since the breakthrough of convolutional neural networks (CNNs) [4, 10, 13, 17, 21, 23, 27, 28, 39, 41, 46]. The recent success of image-text pre-trained Vision Transformers (ViTs) [7, 43], such as CLIP [34], has revitalized the exploration of

* Work is done during internship at Tencent PCG. †Corresponding author (lmwang@nju.edu.cn).

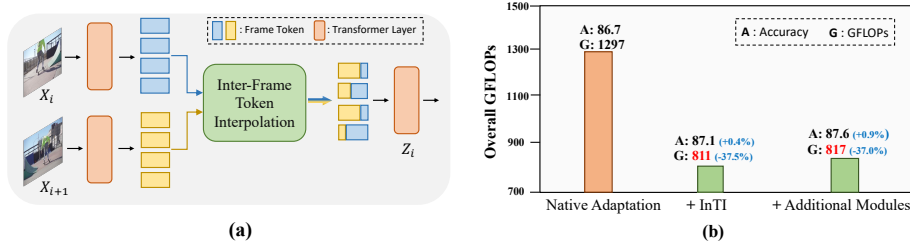


Fig. 1: Overview of InTI and its performance on K400. (a) InTI softly aggregated tokens from neighbor frames with dynamically generated weights. (b) With InTI, we can achieve 87.1% top-1 accuracy with a 37.5% reduction in GFLOPs. InTI can also be combined with any adaptation method, like [18], for better performance.

effective adaptation methods for ViTs [14, 18–20, 24, 25, 30, 31, 33, 36, 42, 48, 50–54, 56, 57].

In this paper, we focus on the efficiency of adaptation methods. Based on whether to introduce new modules during inference, the current approaches can be classified into two types: **1) Extra-cost adaptation**, which introduces additional sophisticated temporal modules, such as learnable prompts [14, 30], temporal convolutions [31, 33, 42], and temporal attention [18, 24, 48, 52, 53, 55], to bridge the domain gap. These modules can be inserted at various positions within the pre-trained image model, including at the end [30], side [18, 24, 25, 33], or in an interleaved way [31, 42, 53]. As performance improves, the inclusion of these additional modules also increases the considerable computational burden during training and inference. **2) Zero-cost adaptation.** By reutilizing [36] or disentangling [20] the original image module, this method incurs no additional cost during inference compared to the naive adaptation [47] of image pre-trained models (i.e., first processing each frame independently and applying average pooling for late fusion). However, this simplicity inevitably leads to inferior performance compared to the first method.

While the design of adaptation modules has been extensively studied, *the spatiotemporal redundancy in the adaptation* of Transformers from image to video remains a critical issue. Most of the aforementioned methods retain the full forward pass for each frame, leading to a high computation overhead for processing videos. Recent approaches [18] employ temporal downsampling, which is composed of a stride 3D-convolution, at the beginning of the network to compress temporal granularity. However, this inflexible operation inevitably leads to performance degradation without additional input. While token merging/pruning methods [3, 5, 6, 22, 32, 44], which dynamically reduce the tokens for each frame, may serve a similar purpose, their irregular token pruning pattern often destroys the coherent spatial structure of each frame.

To address the above issues, we present InTI, as shown in Fig. 1 (a), a novel method for compressive image-to-video adaptation through dynamic **Inter-frame Token Interpolation**. Our InTI aims to preserve the informative tokens softly without disrupting the coherent spatiotemporal structure. Specifically, each to-

ken pair at identical positions in neighbor frames is linearly aggregated into a new token, where the aggregation weights are dynamically generated by a learnable prediction network. For more effective information aggregation, we aim to make the weight prediction process *token-dependent and spatiotemporal-aware*. To enable such flexibility, we design four different lightweight networks to capture contextual information from different scales and fuse them to predict the weights for each token. In this way, the information of neighbor frames can be adaptively compressed point-by-point with spatiotemporal perceiving, effectively reducing the number of processed frames by half each time.

Compared to previous compression methods [3, 6, 18], InTI offers three notable advantages: **1)** InTI enjoys strong *adaptiveness* by dynamically predicted weights, which could perceive the spatiotemporal contextual information to determine the token importance. **2)** InTI *maintains the coherent spatial structure* of frames after each compression due to its point-by-point fusion strategy, which would not interfere with spatial modeling and allow better design flexibility. **3)** InTI *explicitly preserves the feature space* while adaptation, which benefits to transfer of the image pre-trained knowledge and stabilizes the training process.

To evaluate the efficacy of InTI, we apply it to the naive adaptation setting. As illustrated in Fig. 1(b), when employing the ViT-L model on the Kinetics-400 dataset [15], the naive adaptation achieves a top-1 accuracy of 86.7% while consuming 1297 Giga Floating Point Operations (GFLOPs). In contrast, by leveraging InTI, we observe a notable boost in efficiency, reaching an accuracy of **87.1%** while reducing the computational load by a substantial **37.5%** in terms of GFLOPs. This compelling outcome validates the effectiveness of InTI for compressive adaptation of Transformers from images to videos. Further, due to the design flexibility InTI enjoys, we also combined InTI with the temporal modules in [18], and the performance further achieved **87.6%** with a **37%** reduction in GFLOPs compared to the naive adaptation. Similar conclusions have also been verified in the Something-Something V2 dataset [9], further demonstrating the generalizability of InTI.

In summary, our contributions are as follows:

- We present InTI, a novel method for compressive adaptation of Transformers from images to videos, which dynamically aggregates tokens point-by-point from neighbor frames.
- We design four lightweight networks for perceiving contextual information from different spatiotemporal scales to ensure flexibility in weight prediction.
- InTI itself can reach a top-1 accuracy of 87.1% with a remarkable 37.5% reduction in GFLOPs compared to naive adaptation on K400.

2 Related Work

2.1 Transformers for Video Understanding

Currently, there are two main approaches to applying Transformers to video understanding. The first type of method designs video transformer models specifically for video data, either through self-supervised [12, 40, 45] or supervised

training [8, 29], to directly learn the required capabilities for video understanding. However, due to the difficulty in obtaining high-quality video data, these methods often suffer from limited generalization ability [36]. The second type of approach utilizes powerful image-pre-trained models for image-to-video adaptation by designing temporal modules to adapt image models to the domain of videos [2, 26]. For instance, VideoPrompt [14] introduced continuous prompt vectors, ST-Adapter [31] introduced depth-wise 3D convolution layers, and UniFormerV2 [18] redesigned local and global relation aggregators. Recently, ZeroI2V [20] decoupled the original attention mechanism into spatial-temporal dual-headed attention, removing the need for additional overhead. In contrast, our approach considers the redundancy of video data during the adaptation process and proposes dynamic inter-frame token interpolation, which significantly reduces computational costs while achieving comparable performance.

2.2 Efficient Learning with ViTs

There have been several attempts at efficient learning with ViTs in images [3, 5, 22, 35, 37, 49], and most of them focus on effectively pruning/merging tokens. For example, in EViT [22], the relevance between the cls token and other tokens is used to prune tokens, while in ToMe [3], the similarity between tokens is used as an indicator to merge them. Although these image-level methods can be directly applied to each frame, they struggle to consider the temporal information between frames [6]. Recently, some methods specifically designed for videos have been proposed, which attempt to inject temporal information into the process of token pruning and merging [6, 32, 44]. For example, STTS [44] dynamically selects informative tokens in both temporal and spatial dimensions conditioned on video samples. STA [6] proposes the semantic-aware temporal accumulation score to integrally prune spatiotemporal tokens. The key difference between our method and previous works is that the token pruning/selection unavoidably disrupts the coherent spatial structure of frames. In contrast, our method preserves the spatial structure well, which would not interfere with spatial modeling and allows better design flexibility.

3 Method

In this section, we begin by introducing the overview of the methods to adapt image Transformers to video (Sec. 3.1). Subsequently, we define the compressive adaptation for Transformers and present our formulation as a dynamic inter-frame token interpolation (InTI). We also discuss our method compared with token merging/selection and temporal downsampling (Sec. 3.2). Finally, we provide a comprehensive description of the design details in the dynamic inter-frame token interpolation, including multi-scale information extraction and weight prediction (Sec. 3.3).

3.1 Adapting Image Transformers to Video

Due to the strong generalizable prior provided by Vision Transformers (ViTs) [7, 43] pre-trained on image-text tasks, such as CLIP [34], there is a growing interest in adapting these models to the domain of video understanding. To begin with, we describe the forward pass of a single image in ViTs. For an image $I \in \mathbb{R}^{H \times W \times 3}$, ViTs first divide the image into N non-overlapping tokens of equal size, and then concatenate an additional class token for capturing global semantic. The concatenated tokens are denoted as $X_0 \in \mathbb{R}^{(N+1) \times C}$. Then, X_0 sequentially passes through L transformer blocks (let B_l denote the l -th block), and the process can be represented as

$$X_l = B_l(X_{l-1}), \quad (1)$$

where X_l represents the output after l blocks. The class token in the final output X_L receives supervision to learn how to extract semantic information from the image. When adapting the pre-trained image model to the video domain, the simplest approach is to perform naive adaptation, which first processes each frame independently and averages the class tokens at the end, like [36, 47], without any additional parameters. The forward pass of each frame can be expressed as

$$X_l^t = B_l(X_{l-1}^t), \quad (2)$$

where X_l^t represents the output after l blocks for the t -th frame. However, this approach fails to model temporal information between frames. Therefore, most current image-to-video adaptation methods focus on designing additional temporal modeling modules in B , such as learnable prompts [14, 30], temporal convolutions [31, 33, 42], and temporal attention [18, 24, 48, 52, 53]. The overall process can be represented as

$$X_l^t = B_l^{I2V}(X_{l-1}^t, M_t), \quad (3)$$

where B_l^{I2V} represents the l -th block with an additional temporal modeling module for image-to-video adaptation, and M_t represents the additional information, such as neighboring frames or global context, required for temporal modeling centered on X^t . Finally, the class token of each frame is aggregated using average pooling or an additional module, such as an extra transformer layer [30, 33], to obtain the final representation. Some recent works [18, 25, 33] also introduce a separate branch for temporal modeling, while the forward pass of each frame is still preserved to provide pre-trained information.

3.2 Compressive Adaptation with InTI

Based on the aforementioned discussion, to adapt Transformers from images to videos, most of the existing methods would incur a cost of at least T (T denotes the number of frames) times higher than the forward pass of a single image. However, in contrast to images, video data contains a greater redundancy in space-time information [40]. Consequently, existing methods may contain considerable redundant computations during the adaptation process. Motivated by

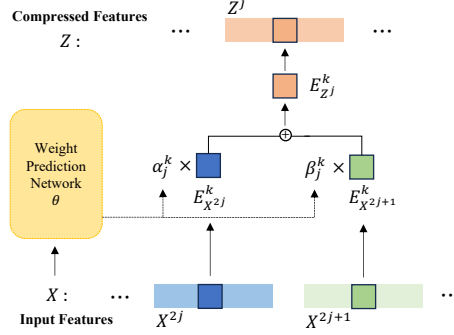


Fig. 2: Illustration of InTI. InTI dynamically aggregates tokens from neighbor frames by a learnable prediction network θ .

this observation, we raise a question: Can we achieve efficient adaptation by compressing the forward pass of each frame? By doing so, under the same total computational cost, we can allocate more resources to temporal modeling.

Compressive Image-to-Video Adaptation. Here we provide a clear definition of how to perform compressive image-to-video adaptation. To ensure that the compression process disentangles from the design of the B_l^{I2V} module, the compression function is inserted between two blocks, therefore the overall process should be represented as:

$$Z_{l-1} = \phi_l(X_{l-1}), \quad (4)$$

$$X_l^t = B_l^{I2V}(Z_{l-1}^t, M_t), \quad (5)$$

where ϕ_l denotes the compression function before the l -th Transformer layer, $X_{l-1} \in \mathbb{R}^{T \times (N+1) \times C}$ denotes input features, and $Z_{l-1} \in \mathbb{R}^{\hat{T} \times (\hat{N}+1) \times C}$ represents the compressed features. The compression function ϕ_l utilizes the information from X_{l-1} to compress either the tokens in each frame ($\hat{N} < N$) or the number of frames ($\hat{T} < T$), thereby compressing the forward pass of each frame. By adjusting the compression frequency, insert position, and the ratio of the compression function, we can easily control the overall degree of compression. For brevity, we omit the subscript l in the following equations.

Inter-frame Token Interpolation (InTI). In this paper, we propose a simple yet effective method, named Inter-frame Token Interpolation (InTI), for compressing the number of frames each time. InTI aims to dynamically preserve the informative tokens while decreasing the redundancy information in spatiotemporal in a soft way. Specifically, InTI compresses the temporal neighbor pairs of frames by aggregating the tokens at identical positions using generated weights. For example, as shown in Fig. 2, for k -th tokens $E_{X^{2j}}^k$ and $E_{X^{2j+1}}^k$ in a pair of frames X^{2j} and X^{2j+1} , to acquire the k -th token $E_{Z^j}^k$ in the j -th compressed frame Z^j , the compression function ϕ can be represented as:

$$\alpha_j^k, \beta_j^k = \theta(X)_j^k, \quad (6)$$

$$E_{Z^j}^k = \alpha_j^k \times E_{X^{2j}}^k + \beta_j^k \times E_{X^{2j+1}}^k, \quad (7)$$

where θ denotes the weight prediction network, which perceives the spatiotemporal contextual information from X and predicts the interpolation weights α and β ($\alpha + \beta = 1$) for each pair of tokens. By generating α_j^k and β_j^k depending on X , the model can adaptively aggregate the information from the two tokens $E_{X^{2j}}^k$ and $E_{X^{2j+1}}^k$ into $E_{Z^j}^k$. $E_{Z^j}^k$ serves to approximate significant information of these two tokens, hence we term the process as “token interpolation”. Ideally, the valuable tokens for video understanding will have larger weights, and the redundant tokens will have smaller weights. As a result, after each inter-frame token interpolation, the information from adjacent frames X^{2j} and X^{2j+1} are dynamically compressed into a single frame point-by-point, effectively halving the number of frames.

Temporal Position Embedding. To enhance the temporal order information in the fused tokens, we incorporate additional temporal embeddings into the tokens before weight prediction and token fusion, as shown below:

$$X = X + \sigma P. \quad (8)$$

Here, σ is a dynamic factor initialized with zero to maintain the stability of the feature distribution at the beginning. $P \in \mathbb{R}^{T \times 1 \times C}$ represents the learnable temporal position embedding.

Comparison to Token Pruning/Merging. Token pruning/merging [3, 5, 6, 22, 32, 44], which reduces the number of tokens in each frame, can also serve as a method for compressing the forward pass. However, our approach offers two significant advantages over them. **Firstly**, token merging-based methods [3, 6] typically require computing the pairwise similarity between every pair of tokens to identify the most similar ones for merging. In contrast, we leverage simply aggregated tokens in the same positions, avoiding unnecessary computations. **What’s more**, token pruning/merging disrupts the coherent spatial structure of each frame because the positions of pruned or merged are irregular. Whereas our point-by-point token interpolation strategy preserves the spatiotemporal structure of the video frames well.

Comparison to Temporal Downsampling. Applying the temporal downsampling at the beginning or middle of the forward pass [18, 26, 40], which employs a lightweight network, like non-overlapping 3D convolutions, to encode each cube region into a token embedding, is another effective approach to reduce the number of frames gradually. However, our method offers a more adaptive and advantageous solution. **Firstly**, InTI explicitly constrains the sum of weights equal to one, which helps preserve the image-pre-trained feature space. In contrast, the temporal downsampling projects tokens into a new linear space by convolutions. Though it can be inflated by pre-trained image weights, it still may disrupt the pre-trained knowledge due to its unconstrained optimization. **Furthermore**, InTI dynamically predicts weights in every position based on the current input sample, allowing for better flexibility. On the other hand, the temporal downsampling is usually shared across different positions and remains fixed after training.

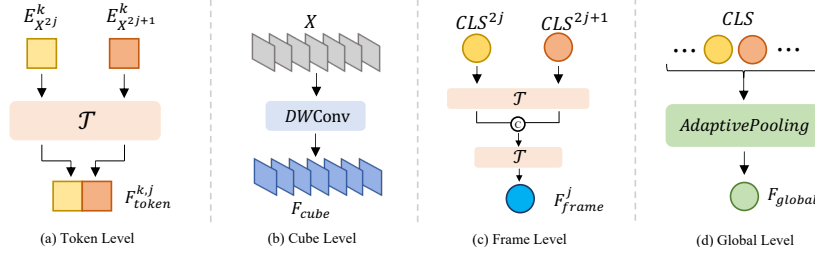


Fig. 3: Multi-Scale Information Extraction. We design four different lightweight networks for capturing contextual information on multiple scales for enhancing the spatiotemporal perception of weight prediction.

3.3 Weight Prediction Network

In this section, we will delve into the specific details of θ in Eq. (6), which extracts multi-scale spatiotemporal context information and utilizes this information to predict the weights.

Multi-Scale Contextual Information Extraction. As shown in Fig. 3, we carefully design four lightweight networks, each corresponding to a specific semantic level, to provide informative contextual features for weight prediction:

(1) Token level: Given k -th tokens $E_{X^{2j}}^k$ and $E_{X^{2j+1}}^k \in \mathbb{R}^C$ in the j -th pair of frames X^{2j} and X^{2j+1} , we compress them to get the token-level representation, as follows:

$$F_{token}^{k,j} = [\mathcal{T}_{C \rightarrow C/2}(E_{X^{2j}}^k), \mathcal{T}_{C \rightarrow C/2}(E_{X^{2j+1}}^k)]. \quad (9)$$

Here, $\mathcal{T}_{C \rightarrow C/2}$ represents a lightweight network composed of a Layer Norm [1], a linear projection that reduces the channel dimension from C to $C/2$, and the GeLU [11] activation function. $[\cdot, \cdot]$ represents the concatenating operation.

(2) Cube level: Capturing local spatiotemporal information around each token is also beneficial for determining token importance. Inspired by [18], we adopt a depth-wise 3D convolution with kernel size 3 to model the spatiotemporal information surrounding each token, represented as:

$$F_{cube} = DWConv(X). \quad (10)$$

(3) Frame level: To better leverage the knowledge from pre-trained image models, we use the class tokens from the two frames X^{2j} and X^{2j+1} to represent the frame-level information. Let CLS^{2j} denote the class token of frame X^{2j} , the frame-level feature can be acquired by:

$$F_{frame}^j = \mathcal{T}_{C \rightarrow C}([\mathcal{T}_{C \rightarrow C/2}(CLS^{2j}), \mathcal{T}_{C \rightarrow C/2}(CLS^{2j+1})]). \quad (11)$$

(4) Global level: To further incorporate long-range spatiotemporal perceiving, we compress the information of class tokens from all frames into a global feature. This can be represented as:

$$F_{global} = AdaptivePooling(CLS). \quad (12)$$

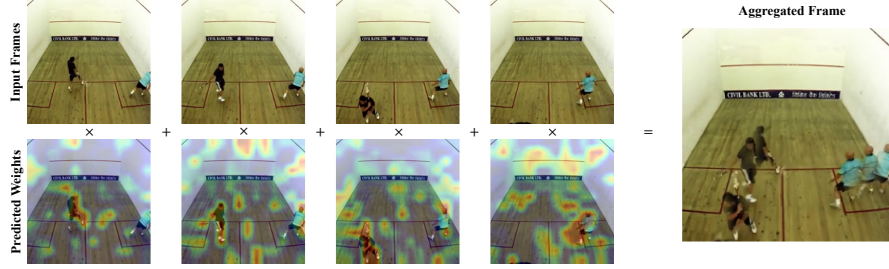


Fig. 4: Visualization of predicted weights and the aggregated frame. As an example, the four frames are compressed twice into a single frame, and the predicted weights for each frame are obtained by cascadedly multiplying the predicted weights at each compression.

Here, AdaptivePooling consists of a few convolutional layers and max pooling (details can be found in the supplementary material). Notable, the global information only needs to be computed once, and then it can be shared by any position, resulting in a small computation overhead on average.

Weight Prediction. Using the information obtained above, we generate the final weights through the following process:

$$\begin{aligned} \alpha_j^k, \beta_j^k &= \text{SoftMax}(\text{FFN}([F_{\text{token}}^{k,j}, F_{\text{context}}^{k,j}])), \\ F_{\text{context}}^{k,j} &= F_{\text{cube}}^{k,j} + F_{\text{frame}}^j + F_{\text{global}}. \end{aligned} \quad (13)$$

We fully retain the token-level information $F_{\text{token}}^{k,j}$ as it is expected to be most relevant to the weight prediction of corresponding tokens. Then, the features of other levels are added up to represent context information $F_{\text{context}}^{k,j}$ (the other design choices are ablated in Sec. 4.3). Finally, $F_{\text{token}}^{k,j}$ and $F_{\text{context}}^{k,j}$ are utilized to generate two logits through two linear layers (FFN), and SoftMax is employed to acquire the final weights. Importantly, the parameters are shared across different spatiotemporal positions, which makes the amount of extra parameters negligible compared to the entire model.

Discussion. To verify that InTI can indeed discriminate the significant tokens, we visualize the predicted weights for four frames along with their corresponding compressed frame, as shown in Fig. 4. The four frames are compressed twice into a single frame, and the predicted weights for each frame are obtained by cascadedly multiplying the weights at each compression. From Fig. 4, we can see that the compressed frame effectively preserves the informative motion trajectory (i.e., two men playing badminton) while maintaining spatial structure integrity. This observation further confirms the capacity of InTI in token importance discrimination. More examples are provided in the supplementary material.

Table 1: Main results on K400. The views of input is $16 \times 3 \times 4$. GFLOPs in the table represent the GFLOPs of a single clip.

Backbones	Methods	GFLOPs	Top1
ViT-B	Naive	281	83.4
	InTI _{3,5}	147 (-48%)	83.6 (+0.2)
	InTI _{5,7}	182 (-35%)	84.1 (+0.7)
	InTI _{7,9}	217 (-23%)	84.2 (+0.8)
	InTI _{3,5} ^{temp}	150 (-47%)	84.5 (+1.1)
	InTI _{5,7} ^{temp}	184 (-35%)	84.9 (+1.5)
	InTI _{7,9} ^{temp}	220 (-22%)	85.0 (+1.6)
ViT-L	Naive	1297	86.7
	InTI _{3,5}	650 (-50%)	86.9 (+0.2)
	InTI _{5,7}	811 (-37%)	87.1 (+0.4)
	InTI _{7,9}	973 (-25%)	87.2 (+0.5)
	InTI _{3,5} ^{temp}	656 (-49%)	87.1 (+0.4)
	InTI _{5,7} ^{temp}	817 (-37%)	87.6 (+0.9)
	InTI _{7,9} ^{temp}	978 (-25%)	87.7 (+1.0)

4 Experiments

4.1 Experimental Setup

Dataset. Our algorithm is primarily evaluated on the popular scene-related dataset named Kinetics400 [15] (K400) and Something-Something V2 [9] (SSv2). Kinetics-400 is a large-scale dataset specifically designed for action recognition tasks and sourced from YouTube. It contains a diverse collection of approximately 10-second video clips, each representing a distinct human action class among the 400 available categories. Something-Something V2 [9] is another popular motion-heavy benchmark with 174 labels. We also provided the results on UCF101 [38] and HMDB51 [16] in the supplementary material.

Implementation Details. In our implementation, we leverage the powerful image-text pre-trained models, the ViTs from CLIP [34], as the image-pre-trained models to investigate compressive adaptation. We refer to the naive adaptation approach of CLIP, which independently processes each frame and applies average pooling for late fusion, as “Naive” in the subsequent experiments. To strike a balance between performance and speed, we incorporate InTI twice during the forward pass of adaptation for all experiments. In this context, InTI_{*i,j*} indicates the insertion of InTI after the *i*-th and *j*-th blocks for ViT-Base, and after the 2*i*-th and 2*j*-th blocks for ViT-Large. Since InTI operates independently from the adaptation method within the blocks, we further introduce the temporal modules in [18], combined with InTI, to further enhance performance. This enhanced approach is denoted as InTI_{*i,j*}^{temp}. Detailed training settings are provided in the supplementary material.

Table 2: Comparison with SOTA methods on the Kinetics-400 dataset. “†” indicates the results obtained by ourselves under the same dataset setting for a fair comparison.

Methods	Views	GFLOPs	Param (M)	Top1	Top5
<i>Extra-cost adaptation</i>					
ST-Adapter-B [31]	$16 \times 1 \times 3$	304	93	82.5	96.0
EVL-B [24]	$16 \times 1 \times 3$	296	115	83.6	-
AIM-B [53]	$16 \times 1 \times 3$	405	97	84.5	96.6
ActionCLIP-B [48]	$16 \times 3 \times 10$	845	142	82.6	96.2
X-CLIP-B [30]	$16 \times 3 \times 4$	287	122	84.7	96.8
X-CLIP-L [30]	$8 \times 3 \times 4$	1316	430	87.1	97.6
UniFormerV2-B† [18]	$16 \times 3 \times 4$	297	115	85.0	96.8
UniFormerV2-L† [18]	$16 \times 3 \times 4$	1332	354	87.5	97.4
<i>Zero-cost adaptation</i>					
ZeroI2V-B [20]	$16 \times 1 \times 3$	281	86	83.4	96.2
ZeroI2V-L [20]	$16 \times 1 \times 3$	1297	304	86.8	97.6
ViFi-CLIP-B [36]	$16 \times 3 \times 4$	281	86	83.9	96.3
Native-B†	$16 \times 3 \times 4$	281	86	83.4	96.2
Native-L†	$16 \times 3 \times 4$	1297	304	86.7	97.2
<i>Compressive adaptation</i>					
ToMe ^{temp} -B† [3]	$16 \times 3 \times 4$	192	115	84.2	96.5
STA ^{temp} -B† [6]	$16 \times 3 \times 4$	192	115	84.1	96.5
ConvPooling _{5,7} ^{temp} -B†	$16 \times 3 \times 4$	184	127	82.7	95.9
LinearPooling _{5,7} ^{temp} -B†	$16 \times 3 \times 4$	179	115	83.9	96.3
InTI ^{temp} -B	$16 \times 3 \times 4$	184	126	84.9	96.8
InTI ^{temp} -L	$16 \times 3 \times 4$	817	378	87.6	97.6

4.2 Main Results

Compressive Image-to-Video Adaptation with InTI. In Tab. 1, we provide comprehensive results regarding computational costs (GFLOPs) and performance on K400 when incorporating InTI at different layers under different backbone scales. Our findings reveal several important insights. **Firstly**, when InTI is applied in the early layers of the network, such as after the 3-th and 5-th layers, it not only achieves a significant reduction of nearly 50% in GFLOPs compared to naive adaptation but also improves the performance marginally. This observation suggests the presence of redundancy in the adaptation process from images to videos. **Moreover**, when InTI is employed in the intermediate layers, specifically after the 5-th and 7-th layers, we observe a further performance improvement. ViT-Base achieves a performance of 84.1%, while ViT-Large reaches 87.1%. Remarkably, these improvements are accompanied by a reduction of approximately 40% in computational cost. As InTI is shifted towards the later layers, such as after the 7th and 9th layers, the performance gains become relatively smaller. This suggests that the pre-trained spatial modeling knowledge necessary for video understanding is already adequately captured near the intermediate layers. **Therefore**, inserting InTI at the intermediate layers strikes a good balance between computational cost and performance. **What’s more**, our conclusion remains consistent even when incorporating an additional adaptation temporal modeling module. As demonstrated in Tab. 1, combined with the temporal modules in [18], we achieve a substantial performance gain of 1.5% in ViT-Base and 0.9% in ViT-Large, while still reducing the GFLOPs by 37% compared to naive adaptation.

Comparison to the State-of-the-Art. First, we would like to emphasize that our method is primarily designed for compressive adaptation from images to videos, rather than aiming to push the performance limits of video understand-

Table 3: Comparison with SOTA methods on the SSv2 dataset. “†” indicates the results obtained by ourselves under the same dataset setting for a fair comparison.

Methods	Views	GFLOPs	Param (M)	Top1
<i>Extra-cost adaptation</i>				
ST-Adapter-B [31]	$16 \times 1 \times 3$	318	93	69.3
EVL-B [24]	$16 \times 1 \times 3$	341	115	61.7
AIM-B [53]	$16 \times 1 \times 3$	416	100	68.1
UniFormerV2-B† [18]	$16 \times 3 \times 4$	371	163	69.5
<i>Zero-cost adaptation</i>				
ZeroI2V-B [20]	$16 \times 1 \times 3$	281	86	69.4
Native-B†	$16 \times 3 \times 4$	281	86	43.6
<i>Compressive adaptation</i>				
ToMe ^{temp} -B† [3]	$16 \times 3 \times 4$	254	163	68.1
STA ^{temp} -B† [6]	$16 \times 3 \times 4$	254	163	68.4
ConvPooling _{5,7} ^{temp} -B†	$16 \times 3 \times 4$	234	175	67.2
LinearPooling _{5,7} ^{temp} -B†	$16 \times 3 \times 4$	221	163	67.6
InTI_{5,7}^{temp}-B	$16 \times 3 \times 4$	234	174	69.3

ing. Due to the lack of experimental results on the compressive image-to-video adaptation of Transformers in the existing literature, we implemented various baseline methods for compressive adaptation ourselves. For a fair comparison, we controlled their GFLOPs to be very close to InTI. These techniques fall into two categories. **1)** Token merging/pruning aims at decreasing the number of tokens in the forward pass. ToMe [3] is a token merging method based on intra-frame similarity, while STA [6] is a token pruning method based on inter-frame similarity. We conducted experiments following the settings described in their papers. **2)** The second category is temporal downsampling, which is commonly used in video classification based on CNNs. Here we also designed two methods: ConvPooling, which employs a set of stride 3D convolutions to replace InTI, and LinearPooling, which learns fixed linearly weighted coefficients for adjacent frames (all tokens shares). From the table, we observe that *InTI achieves the best performance under similar GFLOPs*. Moreover, we find that LinearPooling outperforms ConvPooling, suggesting that *a constrained predicted weight is indeed beneficial for preserving pretraining knowledge and facilitating adaptation*. Interestingly, the performance of token-based methods surpasses that of temporal downsampling considerably, even though the latter has learnable parameters. *This indicates that using token-level design is more suitable for Transformers*. Overall, our method combines the advantages of both categories and achieves a better balance between speed and performance.

In Tab. 2 and Tab. 3, we also compare InTI with the State-of-the-Art (SOTA) methods of extra-cost adaptation, zero-cost adaptation, and compressive adaptation on K400 and SSv2. We observe that adaptation based on InTI achieves *performance comparable to previous methods while significantly reducing computational costs*. For instance, in the case of UniFormerV2 [18] of extra-cost adaptation, we achieve comparable performance on both K400 and SSv2 while reducing GFLOPs by **39%**. Similarly, compared to ZeroI2V [20] of zero-cost

Table 4: Training and inference costs. All results are tested with ViT-Lagre on V100.

Methods	Training (H/Epoch)	Latency (ms)	Top1
UniformerV2† [18]	2.7	240	87.5
Naive	2.5	235	86.7
STA ^{temp} [6]	2.1	195	87.1
InTI_{6,7}^{temp}	2	153	87.6

Table 5: Ablation study.

(a) Ablation on the contextual information from different scales. (b) Ablation on the design choices for weight prediction.

Contextual Information			Param(M)	Top1
F_{cube}	F_{frame}	F_{global}		
			118	84.3
✓			121	84.4
	✓		121	84.6
		✓	121	84.5
✓	✓		124	84.7
	✓	✓	123	84.8
✓	✓	✓	126	84.9

Design	Methods	Param (M)	Top1
Feature Fusion	Add All	125	84.5
	Cat All	128	84.7
	Sep F_{token}	126	84.9
Prediction Head	Sigmoid	126	84.5
	Attention	126	84.6
	Softmax	126	84.9

adaptation, we achieve a performance gain of 0.8% on K400 with a reduction of **37%** in GFLOPs.

Comparison of Training and Inference Costs. In Tab. 4, we compare the training time and testing latency between InTI and different methods under identical hardware conditions. Firstly, among the adaptation methods incurring additional overhead, UniformerV2 [18] is already considered highly efficient, as it only incurs a 10% slowdown compared to naive adaptation. However, our proposed InTI not only achieves a remarkable 26% reduction in training time and 37% in testing latency but also maintains comparable performance. In comparison to naive adaptation, one of the zero-cost methods, InTI not only achieves a performance gain of 0.9% but also reduces training time by 20% and latency by 35%. Lastly, when compared to STA [6], which also serves as a compressive adaptation method, InTI outperforms it by 0.5% in terms of performance and exhibits 22% faster testing latency. These findings further validate the effectiveness of InTI as a compressive adaptation method.

4.3 Ablation Study

In the ablation study, we delve into the effectiveness of different design choices of InTI. All the following experiments are conducted based on the ViT-Base with input views $16 \times 3 \times 4$, and evaluated on the K400 dataset. In the tables, the performance of the default setting is colored gray.

Effect of the Multi-Scale Contextual Information. In Tab. 5a, we explore the effectiveness of spatiotemporal contextual information from different scales.

Firstly, it is worth noting that even with only token-level information (the first row in the table), InTI still achieves promising performance compared to native adaptation (84.3 *vs.* 83.4), which highlights the overall design of InTI. When introducing individual scales of information (rows 1-3 in the table), we observe that frame-level information, obtained through the class token, proves to be the most effective. This suggests that the class token, which captures global semantics during image pretraining, is also helpful in determining the importance of each token, aligning with the assumption of [22]. Furthermore, combining the information from other scales with frame-level information leads to further performance improvements, indicating the effectiveness of cube-level and global-level information. As a result, we incorporate information from all scales as contextual information to predict the weights to maximize the adaptability.

Design Choices for Weight Prediction. In Tab. 5b, we extensively explore the design choices of how to predict the weights. Firstly, we investigate how to fuse the multi-scale contextual features. The “Add All” approach in the table refers to summing all the features into a single feature, while “Cat All” refers to concatenating the features as the final feature. “Sep F_{token} ” indicates preserving token-level information intact and concatenating it with the sum of other scale features. As shown in the first three rows of the table, preserving token-level information proves beneficial for weight prediction of each token, while also reducing the parameter count compared to concatenating all features.

Next, we delve into the design of weight prediction heads. “Sigmoid” denotes the use of the sigmoid function individually on two logits obtained by compressing the contextual features through FFN, without enforcing their sum to be 1. “Attention” involves learning an additional learnable vector for each layer, performing a dot product with each token’s corresponding feature, and then softmax in each pair of tokens. On the other hand, “Softmax” directly applies softmax to the two logits. As shown in the table, the direct softmax approach achieves the best performance. Notably, the sigmoid approach performs the worst, validating our hypothesis that linearly weighted tokens can preserve the feature space knowledge from image pretraining.

5 Conclusion and Future Work

In this work, we have proposed InTI, a novel approach for compressive adaptation of Transformers from images to videos, leveraging inter-frame token interpolation. InTI is designed to preserve informative tokens smoothly while maintaining a coherent spatiotemporal structure. Specifically, InTI conducts compression by aggregating tokens point-by-point within temporal neighbor pairs of frames using linear weights. The weights are dynamically predicted using contextual information from multiple scales. Experimental results demonstrate that InTI effectively compresses information compared to previous methods, achieving state-of-the-art (SOTA) performance when combined with additional adaptation, while significantly reducing computational complexity. Given the efficiency and design flexibility offered by InTI, we believe that integrating the following

advanced image-to-video adaptation methods with InTI can also yield enhanced performance while reducing computational costs. Furthermore, we hope that InTI can serve as an inspiration for more exploration of compressive image-to-video adaptation within various tasks.

A Experiments on UCF101 and HMDB51

As shown in Tab. 7, we have provided additional results on the UCF101 [38] and HMDB51 [16] datasets, and it is evident that our approach demonstrates significant advantages compared to existing compressive adaptation methods and is comparable to uncompressed methods while reducing the significant computational cost.

Table 7: Results on UCF101 and HMDB51.

Methods	GFLOPs	UCF101	HMDB51
<i>Uncompressed adaptation</i>			
UniFormerV2-B† [18]	297	96.4	74.1
ZeroI2V-B [20]	281	95.6	73.7
Native-B†	281	92.3	65.4
<i>Compressive adaptation</i>			
ToMe ^{temp} -B† [3]	192	95.8	72.7
STA ^{temp} -B† [6]	192	95.5	72.9
ConvPooling _{5,7} ^{temp} -B†	184	95.2	72.4
LinearPooling _{5,7} ^{temp} -B†	179	94.4	71.2
InTI _{5,7} ^{temp} -B	184	96.4	74.0

B Global-level Information Extraction

The detailed structure of the global-level information extraction network is as follows: Firstly, we pass all class tokens CLS through a 1D temporal convolution with kernel size 3 and stride 1. Subsequently, we apply max pooling with stride 2 and the GELU activation. Then the above three modules are repeated again to further reduce the temporal length. Finally, another 1D convolution layer with kernel size 3 and stride 1, a global average layer, and another GELU activation are used to obtain the F_{global} . For efficiency, all convolutions are depth-wise.

C More Visualizations

In Fig. 5, we provide more visualizations about the predicted weights and the aggregated frame. Compared to directly averaging the frames, InTI successfully captures the significant tokens in each frame and softly aggregates them into the fused frame, while maintaining the spatiotemporal structure.

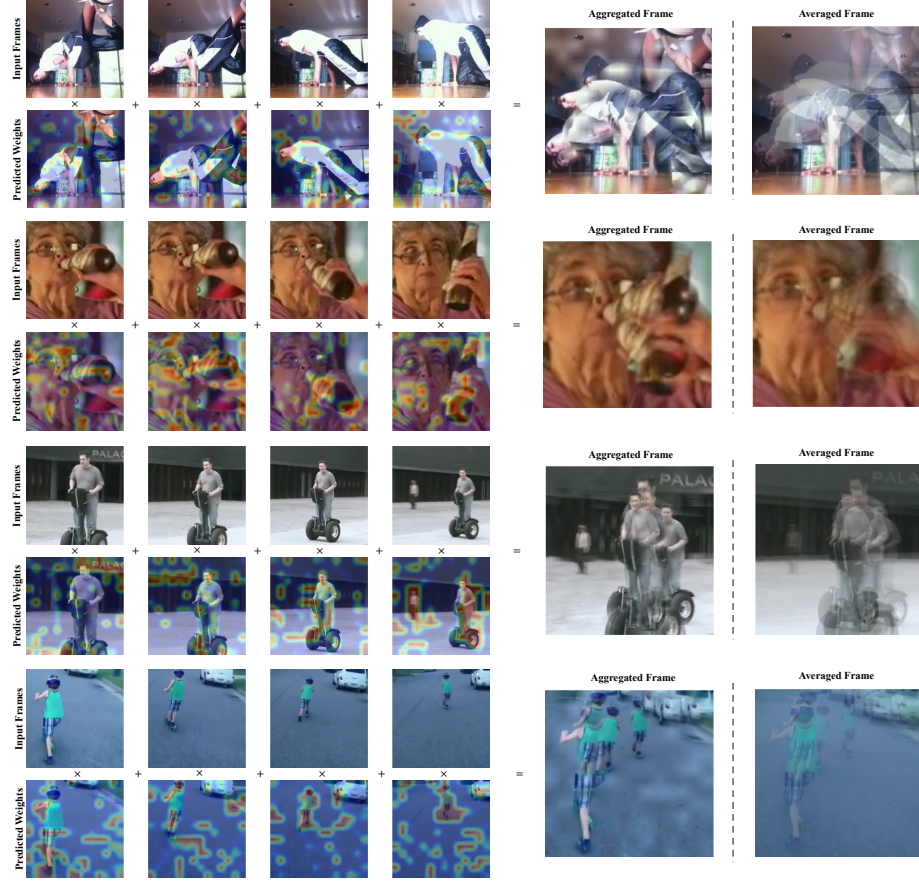


Fig. 5: Additional visualization of predicted weights and the aggregated frame. Each four frames is compressed twice into a single frame, and the predicted weights for each frame are obtained by cascadedly multiplying the predicted weights at each compression.

D Training Details

For Kinetics-400 [15], all our experiments follow the full fine-tuned setting in [36] except we don't use the text encoder of CLIP. For SSv2 [9], our setting closely adheres to the configuration in [18], with the exception that we reduce the batch size from 128 to 64 for ViT-B due to resource constraints.

References

1. Ba, J.L., Kiros, J.R., Hinton, G.E.: Layer normalization. arXiv preprint arXiv:1607.06450 (2016) 8
2. Bertasius, G., Wang, H., Torresani, L.: Is space-time attention all you need for video understanding? In: Meila, M., Zhang, T. (eds.) International Conference on Machine Learning. Proceedings of Machine Learning Research, vol. 139, pp. 813–824. PMLR (2021), <http://proceedings.mlr.press/v139/bertasius21a.html> 4
3. Bolya, D., Fu, C.Y., Dai, X., Zhang, P., Feichtenhofer, C., Hoffman, J.: Token merging: Your vit but faster. In: International Conference on Learning Representations (2022) 2, 3, 4, 7, 11, 12, 15
4. Carreira, J., Zisserman, A.: Quo vadis, action recognition? a new model and the kinetics dataset. In: Proceedings of the IEEE/CVF International Conference on Computer Vision. pp. 6299–6308 (2017) 1
5. Chen, M., Shao, W., Xu, P., Lin, M., Zhang, K., Chao, F., Ji, R., Qiao, Y., Luo, P.: Diffrate: Differentiable compression rate for efficient vision transformers. arXiv preprint arXiv:2305.17997 (2023) 2, 4, 7
6. Ding, S., Zhao, P., Zhang, X., Qian, R., Xiong, H., Tian, Q.: Prune spatio-temporal tokens by semantic-aware temporal accumulation. In: Proceedings of the IEEE/CVF International Conference on Computer Vision. pp. 16945–16956 (2023) 2, 3, 4, 7, 11, 12, 13, 15
7. Dosovitskiy, A., Beyer, L., Kolesnikov, A., Weissenborn, D., Zhai, X., Unterthiner, T., Dehghani, M., Minderer, M., Heigold, G., Gelly, S., et al.: An image is worth 16x16 words: Transformers for image recognition at scale. In: International Conference on Learning Representations (2020) 1, 5
8. Fan, H., Xiong, B., Mangalam, K., Li, Y., Yan, Z., Malik, J., Feichtenhofer, C.: Multiscale vision transformers. In: Proceedings of the IEEE/CVF International Conference on Computer Vision. pp. 6824–6835 (2021) 4
9. Goyal, R., Ebrahimi Kahou, S., Michalski, V., Materzynska, J., Westphal, S., Kim, H., Haenel, V., Fruend, I., Yianilos, P., Mueller-Freitag, M., et al.: The "something something" video database for learning and evaluating visual common sense. In: Proceedings of the IEEE/CVF International Conference on Computer Vision. pp. 5842–5850 (2017) 3, 10, 17
10. He, D., Zhou, Z., Gan, C., Li, F., Liu, X., Li, Y., Wang, L., Wen, S.: Stnet: Local and global spatial-temporal modeling for action recognition. In: Proceedings of the AAAI conference on artificial intelligence. vol. 33, pp. 8401–8408 (2019) 1
11. Hendrycks, D., Gimpel, K.: Gaussian error linear units (gelus). arXiv preprint arXiv:1606.08415 (2016) 8
12. Huang, B., Zhao, Z., Zhang, G., Qiao, Y., Wang, L.: Mgmoe: Motion guided masking for video masked autoencoding. In: Proceedings of the IEEE/CVF International Conference on Computer Vision. pp. 13493–13504 (2023) 3

13. Jiang, B., Wang, M., Gan, W., Wu, W., Yan, J.: Stm: Spatiotemporal and motion encoding for action recognition. In: *Proceedings of the IEEE/CVF International Conference on Computer Vision*. pp. 2000–2009 (2019) [1](#)
14. Ju, C., Han, T., Zheng, K., Zhang, Y., Xie, W.: Prompting visual-language models for efficient video understanding. In: *European Conference on Computer Vision*. pp. 105–124. Springer (2022) [2](#), [4](#), [5](#)
15. Kay, W., Carreira, J., Simonyan, K., Zhang, B., Hillier, C., Vijayanarasimhan, S., Viola, F., Green, T., Back, T., Natsev, P., et al.: The kinetics human action video dataset. *arXiv preprint arXiv:1705.06950* (2017) [3](#), [10](#), [17](#)
16. Kuehne, H., Jhuang, H., Garrote, E., Poggio, T., Serre, T.: Hmdb: a large video database for human motion recognition. In: *ICCV*. pp. 2556–2563. IEEE (2011) [10](#), [15](#)
17. Kwon, H., Kim, M., Kwak, S., Cho, M.: Motionsqueeze: Neural motion feature learning for video understanding. In: *European Conference on Computer Vision*. pp. 345–362. Springer (2020) [1](#)
18. Li, K., Wang, Y., He, Y., Li, Y., Wang, Y., Wang, L., Qiao, Y.: Uniformerv2: Unlocking the potential of image vits for video understanding. In: *Proceedings of the IEEE/CVF International Conference on Computer Vision*. pp. 1632–1643 (2023) [2](#), [3](#), [4](#), [5](#), [7](#), [8](#), [10](#), [11](#), [12](#), [13](#), [15](#), [17](#)
19. Li, X., Huang, Z., Wang, J., Li, K., Wang, L.: Videoeval: Comprehensive benchmark suite for low-cost evaluation of video foundation model. *arXiv preprint arXiv:2407.06491* (2024) [2](#)
20. Li, X., Wang, L.: Zeroi2v: Zero-cost adaptation of pre-trained transformers from image to video. *arXiv preprint arXiv:2310.01324* (2023) [2](#), [4](#), [11](#), [12](#), [15](#)
21. Li, Y., Ji, B., Shi, X., Zhang, J., Kang, B., Wang, L.: Tea: Temporal excitation and aggregation for action recognition. In: *Proceedings of the IEEE/CVF International Conference on Computer Vision*. pp. 909–918 (2020) [1](#)
22. Liang, Y., Chongjian, G., Tong, Z., Song, Y., Wang, J., Xie, P.: Evit: Expediting vision transformers via token reorganizations. In: *International Conference on Learning Representations* (2021) [2](#), [4](#), [7](#), [14](#)
23. Lin, J., Gan, C., Han, S.: Tsm: Temporal shift module for efficient video understanding. In: *Proceedings of the IEEE/CVF International Conference on Computer Vision*. pp. 7083–7093 (2019) [1](#)
24. Lin, Z., Geng, S., Zhang, R., Gao, P., de Melo, G., Wang, X., Dai, J., Qiao, Y., Li, H.: Frozen clip models are efficient video learners. In: *European Conference on Computer Vision*. pp. 388–404. Springer (2022) [2](#), [5](#), [11](#), [12](#)
25. Liu, R., Huang, J., Li, G., Feng, J., Wu, X., Li, T.H.: Revisiting temporal modeling for clip-based image-to-video knowledge transferring. In: *Proceedings of the IEEE/CVF International Conference on Computer Vision*. pp. 6555–6564 (2023) [2](#), [5](#)
26. Liu, Z., Ning, J., Cao, Y., Wei, Y., Zhang, Z., Lin, S., Hu, H.: Video swin transformer. In: *Proceedings of the IEEE/CVF International Conference on Computer Vision*. pp. 3202–3211 (2022) [4](#), [7](#)
27. Liu, Z., Luo, D., Wang, Y., Wang, L., Tai, Y., Wang, C., Li, J., Huang, F., Lu, T.: Teinet: Towards an efficient architecture for video recognition. In: *Proceedings of the AAAI conference on artificial intelligence*. vol. 34, pp. 11669–11676 (2020) [1](#)
28. Liu, Z., Wang, L., Wu, W., Qian, C., Lu, T.: Tam: Temporal adaptive module for video recognition. In: *Proceedings of the IEEE/CVF International Conference on Computer Vision*. pp. 13708–13718 (2021) [1](#)

29. Neimark, D., Bar, O., Zohar, M., Asselmann, D.: Video transformer network. In: Proceedings of the IEEE/CVF International Conference on Computer Vision. pp. 3163–3172 (2021) [4](#)
30. Ni, B., Peng, H., Chen, M., Zhang, S., Meng, G., Fu, J., Xiang, S., Ling, H.: Expanding language-image pretrained models for general video recognition. In: European Conference on Computer Vision. pp. 1–18. Springer (2022) [2](#), [5](#), [11](#)
31. Pan, J., Lin, Z., Zhu, X., Shao, J., Li, H.: St-adapter: Parameter-efficient image-to-video transfer learning. *Advances in Neural Information Processing Systems* **35**, 26462–26477 (2022) [2](#), [4](#), [5](#), [11](#), [12](#)
32. Park, S.H., Tack, J., Heo, B., Ha, J.W., Shin, J.: K-centered patch sampling for efficient video recognition. In: European Conference on Computer Vision. pp. 160–176. Springer (2022) [2](#), [4](#), [7](#)
33. Qing, Z., Zhang, S., Huang, Z., Zhang, Y., Gao, C., Zhao, D., Sang, N.: Disentangling spatial and temporal learning for efficient image-to-video transfer learning. In: Proceedings of the IEEE/CVF International Conference on Computer Vision. pp. 13934–13944 (2023) [2](#), [5](#)
34. Radford, A., Kim, J.W., Hallacy, C., Ramesh, A., Goh, G., Agarwal, S., Sastry, G., Askell, A., Mishkin, P., Clark, J., et al.: Learning transferable visual models from natural language supervision. In: International Conference on Machine Learning. pp. 8748–8763. PMLR (2021) [1](#), [5](#), [10](#)
35. Rao, Y., Zhao, W., Liu, B., Lu, J., Zhou, J., Hsieh, C.J.: Dynamicvit: Efficient vision transformers with dynamic token sparsification. *Advances in Neural Information Processing Systems* **34**, 13937–13949 (2021) [4](#)
36. Rasheed, H., Khattak, M.U., Maaz, M., Khan, S., Khan, F.S.: Fine-tuned clip models are efficient video learners. In: Proceedings of the IEEE/CVF International Conference on Computer Vision. pp. 6545–6554 (2023) [2](#), [4](#), [5](#), [11](#), [17](#)
37. Ryoo, M., Piergiovanni, A., Arnab, A., Dehghani, M., Angelova, A.: Tokenlearner: Adaptive space-time tokenization for videos. *Advances in Neural Information Processing Systems* **34**, 12786–12797 (2021) [4](#)
38. Soomro, K., Zamir, A.R., Shah, M.: Ucf101: A dataset of 101 human actions classes from videos in the wild. *arXiv preprint arXiv:1212.0402* (2012) [10](#), [15](#)
39. Sun, S., Kuang, Z., Sheng, L., Ouyang, W., Zhang, W.: Optical flow guided feature: A fast and robust motion representation for video action recognition. In: Proceedings of the IEEE/CVF International Conference on Computer Vision. pp. 1390–1399 (2018) [1](#)
40. Tong, Z., Song, Y., Wang, J., Wang, L.: Videomae: Masked autoencoders are data-efficient learners for self-supervised video pre-training. *Advances in Neural Information Processing Systems* **35**, 10078–10093 (2022) [3](#), [5](#), [7](#)
41. Tran, D., Wang, H., Torresani, L., Ray, J., LeCun, Y., Paluri, M.: A closer look at spatiotemporal convolutions for action recognition. In: Proceedings of the IEEE/CVF International Conference on Computer Vision. pp. 6450–6459 (2018) [1](#)
42. Tu, S., Dai, Q., Wu, Z., Cheng, Z.Q., Hu, H., Jiang, Y.G.: Implicit temporal modeling with learnable alignment for video recognition. *arXiv preprint arXiv:2304.10465* (2023) [2](#), [5](#)
43. Vaswani, A., Shazeer, N., Parmar, N., Uszkoreit, J., Jones, L., Gomez, A.N., Kaiser, Ł., Polosukhin, I.: Attention is all you need. *Advances in Neural Information Processing Systems* **30** (2017) [1](#), [5](#)
44. Wang, J., Yang, X., Li, H., Liu, L., Wu, Z., Jiang, Y.G.: Efficient video transformers with spatial-temporal token selection. In: European Conference on Computer Vision. pp. 69–86. Springer (2022) [2](#), [4](#), [7](#)

45. Wang, L., Huang, B., Zhao, Z., Tong, Z., He, Y., Wang, Y., Wang, Y., Qiao, Y.: Videomae v2: Scaling video masked autoencoders with dual masking. In: Proceedings of the IEEE/CVF International Conference on Computer Vision. pp. 14549–14560 (2023) [3](#)
46. Wang, L., Tong, Z., Ji, B., Wu, G.: Tdn: Temporal difference networks for efficient action recognition. In: Proceedings of the IEEE/CVF International Conference on Computer Vision. pp. 1895–1904 (2021) [1](#)
47. Wang, L., Xiong, Y., Wang, Z., Qiao, Y., Lin, D., Tang, X., Gool, L.V.: Temporal segment networks: Towards good practices for deep action recognition. In: European Conference on Computer Vision. pp. 20–36 (2016) [2](#), [5](#)
48. Wang, M., Xing, J., Liu, Y.: Actionclip: A new paradigm for video action recognition. arXiv preprint arXiv:2109.08472 (2021) [2](#), [5](#), [11](#)
49. Wang, Y., Huang, R., Song, S., Huang, Z., Huang, G.: Not all images are worth 16x16 words: Dynamic transformers for efficient image recognition. *Advances in Neural Information Processing Systems* **34**, 11960–11973 (2021) [4](#)
50. Weng, Z., Yang, X., Li, A., Wu, Z., Jiang, Y.G.: Transforming clip to an open-vocabulary video model via interpolated weight optimization. arXiv preprint arXiv:2302.00624 (2023) [2](#)
51. Wu, W., Song, Y., Sun, Z., Wang, J., Xu, C., Ouyang, W.: What can simple arithmetic operations do for temporal modeling? In: Proceedings of the IEEE/CVF International Conference on Computer Vision. pp. 13712–13722 (2023) [1](#), [2](#)
52. Wu, W., Sun, Z., Ouyang, W.: Revisiting classifier: Transferring vision-language models for video recognition. In: Proceedings of the AAAI conference on artificial intelligence. vol. 37, pp. 2847–2855 (2023) [2](#), [5](#)
53. Yang, T., Zhu, Y., Xie, Y., Zhang, A., Chen, C., Li, M.: Aim: Adapting image models for efficient video action recognition. In: International Conference on Learning Representations (2022) [2](#), [5](#), [11](#), [12](#)
54. Zhang, G., Liu, C., Cui, Y., Zhao, X., Ma, K., Wang, L.: Vfimamba: Video frame interpolation with state space models. arXiv preprint arXiv:2407.02315 (2024) [2](#)
55. Zhang, G., Zhu, Y., Wang, H., Chen, Y., Wu, G., Wang, L.: Extracting motion and appearance via inter-frame attention for efficient video frame interpolation. In: Proceedings of the IEEE/CVF Conference on Computer Vision and Pattern Recognition. pp. 5682–5692 (2023) [2](#)
56. Zhu, Y., Ji, Y., Zhao, Z., Wu, G., Wang, L.: Awt: Transferring vision-language models via augmentation, weighting, and transportation. arXiv preprint arXiv:2407.04603 (2024) [2](#)
57. Zhu, Y., Zhang, G., Tan, J., Wu, G., Wang, L.: Dual detr for multi-label temporal action detection. In: Proceedings of the IEEE/CVF Conference on Computer Vision and Pattern Recognition. pp. 18559–18569 (2024) [2](#)